

---

# Compress Guidance in Conditional Diffusion Sampling

---

**Anh-Dung Dinh**  
School of Computer Science  
The University of Sydney  
dinhanhdung1996@gmail.com

**Daochang Liu**  
School of Computer Science  
The University of Sydney  
daochang.liu@sydney.edu.au

**Chang Xu \***  
School of Computer Science  
The University of Sydney  
c.xu@sydney.edu.au

## Abstract

Enforcing guidance throughout the entire sampling process often proves counterproductive due to the model-fitting issue, where samples are 'tuned' to match the classifier's parameters rather than generalizing the expected condition. This work identifies and quantifies the problem, demonstrating that reducing or excluding guidance at numerous timesteps can mitigate this issue. By distributing the guidance densely in the early stages of the process, we observe a significant improvement in image quality and diversity while also reducing the required guidance timesteps by nearly 40%. This approach addresses a major challenge in applying guidance effectively to generative tasks. Consequently, our proposed method, termed Compress Guidance, allows for the exclusion of a substantial number of guidance timesteps while still surpassing baseline models in image quality. We validate our approach through benchmarks on label-conditional and text-to-image generative tasks across various datasets and models.

## 1 Introduction

Guidance in diffusion models is mainly divided into classifier-free guidance [1] and classifier guidance [2]. Although both of these methods significantly improve the performance of the diffusion samples [2, 1, 3–5], they both suffer from large computation time. For classifier guidance, the act of gradients calculation backwards through a classifier is costly. On the other hand, forwarding through a diffusion model twice at every timestep also costs significant computation in classifier-free guidance.

This exorbitant process seems to be quite unnecessary. In Figure 1, we show that our work can achieve better image quality with much less time for guidance, hence less sampling time in general. To come up with this solution, we start to investigate the vanilla guidance in the figures in Table 1. We visualize the loss of the guidance classifier during the sampling process. We name this guidance loss as an on-sampling loss (blue line). This indicates that the guidance is mainly useful in the early stage of the sampling process, where the image does not have a clear form of information. In the later stage, where the model focuses more on improving the details of the image, the guidance loss is likely to be close to 0 most of the time. This leaves us questioning whether guidance is necessary for all the timesteps.

By further investigating the image quality during the guidance sampling, we realize that forcing guidance for every time step can cause weird features as the top row in Figure 2. We define a problem

---

\*Corresponding authors

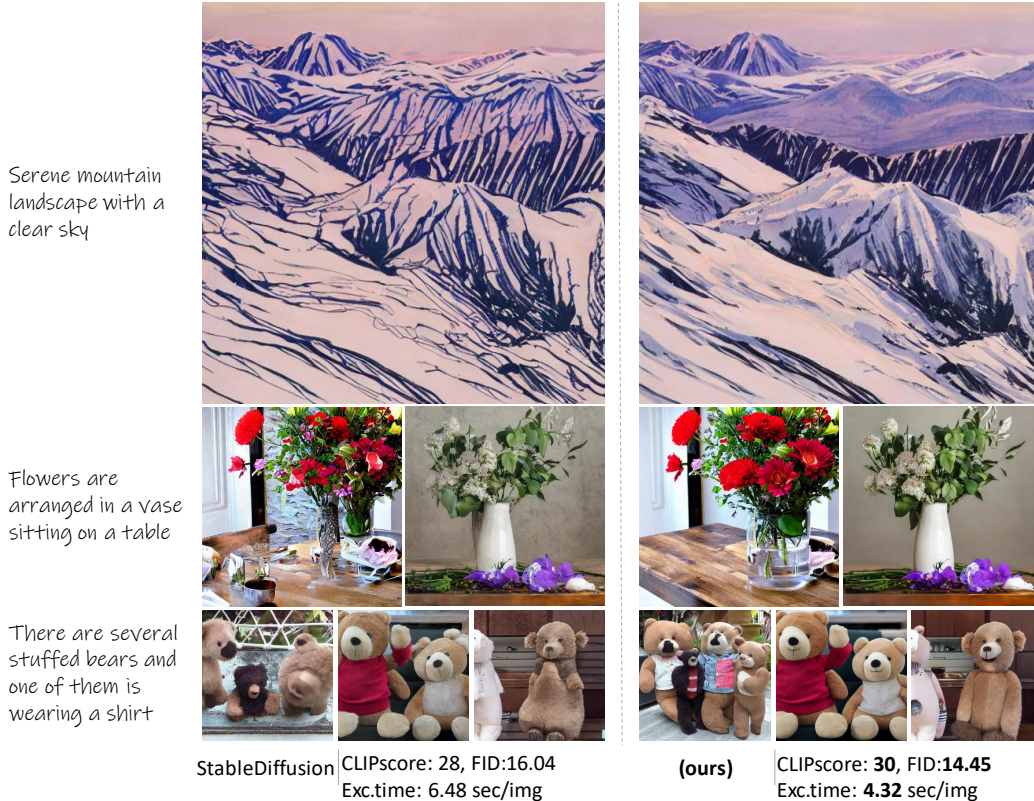


Figure 1: *Stable Diffusion with classifier-free guidance. The left figure is the vanilla classifier-free guidance with application on all 50 timesteps. Our proposed Compress Guidance method is the right figure, where we only apply guidance on 10 over 50 steps. The output shows our methods’ superiority over classifier-free guidance regarding image quality, quantitative performance and efficiency. The efficiency is counted based on the time to generate 30000 images with 1 GPU.*

named **model-fitting**, where image pixels are generated to satisfy the classifier’s features instead of generalizing the information of the expected conditions.

To validate the hypothesis, we provide evidence of model-fitting through loss and accuracy observation. After that, a simple method named Compress Guidance (CompG) is proposed to alleviate the problem by reducing the number of timesteps of calling guidance. This method provides better sample quality and a significantly faster running time.

Overall, the contributions of our works are three-fold: **(1)** Explore and quantify the model-fitting problem in guidance and the wasteful computation resulting from current guidance methods. **(2)** Propose a simple but effective method to contain the model-fitting problem and improve computational time. **(3)** Extensive analysis and experimental results for different datasets and generative tasks on both classifier and classifier-free guidance perspectives.

## 2 Background

**Diffusion Models** [6] has the form of:  $p_\theta := p(\mathbf{x}_T) \prod_{t=1}^T p_\theta(\mathbf{x}_{t-1}|\mathbf{x}_t)$  where  $p_\theta(\mathbf{x}_{t-1}|\mathbf{x}_t) := \mathcal{N}(\mathbf{x}_{t-1}; \mu_\theta(x_t, t), \Sigma_\theta(x_t, t))$  supporting the reverse process from  $\mathbf{x}_T$  to  $\mathbf{x}_0$ . This process is denoising process where starting from the  $\mathbf{x}_T \sim \mathcal{N}(\mathbf{x}_T; 0, \mathbf{I})$  to gradually move to  $\mathbf{x}_0 \sim q(\mathbf{x}_0)$ . This process is trained to be matched with the forward diffusion process  $q(\mathbf{x}_{1:T}|\mathbf{x}_0) := \prod_{t=1}^T q(\mathbf{x}_t|\mathbf{x}_{t-1})$  given  $q(\mathbf{x}_t|\mathbf{x}_{t-1})$  as  $q(\mathbf{x}_t|\mathbf{x}_{t-1}) := \mathcal{N}(\mathbf{x}_t; \sqrt{1 - \beta_t}\mathbf{x}_{t-1}, \beta_t\mathbf{I})$  or we can write the conditional distribution of  $\mathbf{x}_t$  given  $\mathbf{x}_0$  as below:

$$q(\mathbf{x}_t|\mathbf{x}_0) := \mathcal{N}(\mathbf{x}_t; \sqrt{\bar{\alpha}_t}\mathbf{x}_0, (1 - \bar{\alpha}_t)\mathbf{I}) \quad (1)$$

$\beta_t$  is the fixed variance scheduled before the process starts, [6] denotes  $\alpha_t := 1 - \beta_t$  and  $\bar{\alpha}_t := \prod_{s=1}^t \alpha_s$  used in Eq.1. We have the  $\mathbf{x}_{t-1}$  conditioned on  $\mathbf{x}_0$  and  $\mathbf{x}_t$  as:

$$q(\mathbf{x}_{t-1}|\mathbf{x}_t, \mathbf{x}_0) = \mathcal{N}(\mathbf{x}_{t-1}; \tilde{\boldsymbol{\mu}}_t(\mathbf{x}_t, \mathbf{x}_0), \tilde{\beta}_t \mathbf{I}) \quad (2)$$

where  $\tilde{\boldsymbol{\mu}}_t(\mathbf{x}_t, \mathbf{x}_0) := \frac{\sqrt{\bar{\alpha}_{t-1}}\beta_t}{1-\bar{\alpha}_t} \mathbf{x}_0 + \frac{\sqrt{\alpha_t}(1-\bar{\alpha}_{t-1})}{1-\bar{\alpha}_t} \mathbf{x}_t$  and  $\tilde{\beta}_t := \frac{1-\bar{\alpha}_{t-1}}{1-\bar{\alpha}_t} \beta_t$ . To train the diffusion model, the lower bound loss is utilized as below:

$$\mathbb{E}[-\log p_\theta(\mathbf{x}_0)] \leq \mathbb{E}_q[-\log p(\mathbf{x}_T) - \sum_{t \geq 1} \log \frac{p_\theta(\mathbf{x}_{t-1}|\mathbf{x}_t)}{q(\mathbf{x}_t|\mathbf{x}_{t-1})}] \quad (3)$$

Rewrite Eq. 3 as  $\mathbb{E}_q[D_{KL}(q(\mathbf{x}_T|\mathbf{x}_0)||p(\mathbf{x}_T)) + \sum_{t \geq 1} D_{KL}(q(\mathbf{x}_{t-1}|\mathbf{x}_t, \mathbf{x}_0)||p_\theta(\mathbf{x}_{t-1}|\mathbf{x}_t)) - \log p_\theta(\mathbf{x}_0|\mathbf{x}_1)]$  The training process actually optimize the  $\sum_{t \geq 1} D_{KL}(q(\mathbf{x}_{t-1}|\mathbf{x}_t, \mathbf{x}_0)||p_\theta(\mathbf{x}_{t-1}|\mathbf{x}_t))$  where the diffusion model try to match the distribution of  $\mathbf{x}_{t-1}$  by using only  $\mathbf{x}_t$ . There are several implementations for optimising the 3. However, the  $\theta$  as parameters of the noise predictor  $\epsilon_\theta(\mathbf{x}_t, t)$  is the most popular choice. After the  $\theta$  are trained using Eq. 3, the sampling equation:

$$\mathbf{x}_{t-1} = \frac{1}{\sqrt{\alpha_t}} \left( \mathbf{x}_t - \frac{1-\alpha_t}{\sqrt{1-\bar{\alpha}_t}} \epsilon_\theta(\mathbf{x}_t, t) \right) + \sigma_t \mathbf{z} \quad (4)$$

**Guidance** in the Diffusion model offers conditional information and image quality enhancement. Given a classifier  $p_\phi(y|\mathbf{x}_t)$  that match with the labels distribution conditioned on images  $\mathbf{x}_t$ , we have the sampling equation with guidance as:

$$\mathbf{x}_{t-1} \sim \mathcal{N}(\boldsymbol{\mu}_t + s\sigma_t^2 \nabla_{\mathbf{x}_t} \log p_\phi(y|\mathbf{x}_t), \sigma_t) \quad (5)$$

Beside the classifier guidance as Eq.5, [1] proposes another version named classifier-free guidance. This guidance method does not base the information on a classifier. Instead, the guidance depends on the conditional information from a conditional diffusion model. The sampling equation has the form:

$$\mathbf{x}_{t-1} \sim \mathcal{N}(\tilde{\boldsymbol{\mu}}_t(\mathbf{x}_t, \frac{\mathbf{x}_t - \sqrt{1-\bar{\alpha}_t} \tilde{\epsilon}}{\sqrt{\bar{\alpha}_t}}), \sigma_t) \quad (6)$$

given  $\tilde{\epsilon} = (1+w)\epsilon_\theta(\mathbf{x}_t, c) - w\epsilon_\theta(\mathbf{x}_t)$

### 3 Model-fitting in Guidance

We first model the sampling equation into two optimization objectives to show the sampling process is a "training" process to optimize parameters  $\mathbf{x}_t$  over  $T$  timesteps. After that, The observation is conducted on the process of  $\mathbf{x}_t$  "training" given the mentioned objectives and points out the model-fitting problem that the current sampling process with guidance suffers from. Finally, a simple method named Compress Guidance is proposed to alleviate the observed model-fitting. From Eq.4, we have:

$$\mathbf{x}_{t-1} = \frac{(1-\alpha_t)\sqrt{\bar{\alpha}_{t-1}}}{1-\bar{\alpha}_t} \frac{\mathbf{x}_t - \sqrt{1-\bar{\alpha}_t} \epsilon_\theta(\mathbf{x}_t, t)}{\sqrt{\bar{\alpha}_t}} + \frac{(1-\bar{\alpha}_{t-1})\sqrt{\alpha_t}}{1-\bar{\alpha}_t} \mathbf{x}_t + \sigma_t \mathbf{z} \quad (7)$$

**Distribution matching objective:** Assuming that  $\epsilon_\theta(\mathbf{x}_t, t)$  is learned perfectly to match random noise  $\epsilon$  at timestep  $t$ , we have  $\frac{\mathbf{x}_t - \sqrt{1-\bar{\alpha}_t} \epsilon_\theta(\mathbf{x}_t, t)}{\sqrt{\bar{\alpha}_t}} = \mathbf{x}_0$  is the exact prediction of  $\mathbf{x}_0$  at timestep  $t$  according to Eq.1. With  $\tilde{\mathbf{x}}_0$  is the prediction of  $\mathbf{x}_0$  at timestep  $t$ , we can re-write the equation as bellow:

$$\mathbf{x}_{t-1} = \frac{(1-\alpha_t)\sqrt{\bar{\alpha}_{t-1}}}{1-\bar{\alpha}_t} \tilde{\mathbf{x}}_0 + \frac{(1-\bar{\alpha}_{t-1})\sqrt{\alpha_t}}{1-\bar{\alpha}_t} \mathbf{x}_t + \sigma_t \mathbf{z} \quad (8)$$

This equation 8 can be derived from  $q(\mathbf{x}_{t-1}|\mathbf{x}_t, \mathbf{x}_0)$  in Eq. 2 with parameterized trick for Gaussian Distribution. Thus, the first aim of the sampling process is to match the distribution  $q(\mathbf{x}_{t-1}|\mathbf{x}_t, \mathbf{x}_0)$ . Nevertheless, the Eq.8 is based on the assumption that  $\tilde{\mathbf{x}}_0 \sim \mathbf{x}_0$ , which often does not hold when  $t \rightarrow T$ . Given  $\tilde{\mathbf{x}}_0 = \frac{\mathbf{x}_t - \sqrt{1-\bar{\alpha}_t} \epsilon_\theta(\mathbf{x}_t, t)}{\sqrt{\bar{\alpha}_t}}$ , this formulation is rooted from  $\tilde{\mathbf{x}}_0 \sim \mathcal{N}(\frac{1}{\sqrt{\bar{\alpha}}} \mathbf{x}_t; \frac{\bar{\alpha}-1}{\bar{\alpha}} \mathbf{I})$  with assumption that  $\epsilon_\theta(\mathbf{x}_t, t) \sim \epsilon$ . However,  $\epsilon_\theta(\mathbf{x}_t, t)$  is trained to minimize  $D_{KL}[q(\mathbf{x}_{t-1}|\mathbf{x}_t, \mathbf{x}_0)||p_\theta(\mathbf{x}_{t-1}|\mathbf{x}_t)]$  [6] which actually causes a significantly distorted information if  $\epsilon_\theta(\mathbf{x}_t, t)$  is utilized to sample  $\tilde{\mathbf{x}}_0$  from  $\mathbf{x}_t$  if  $t \rightarrow T$ . A smaller  $t$  would result in a better prediction of  $\mathbf{x}_0$  and with  $t = 0$ , we have  $\bar{\alpha} = 1$  resulting in  $\tilde{\mathbf{x}}_0 = \mathbf{x}_t$ .

**Theorem 1.** Assume that  $\epsilon_\theta$  is trained to converge and the real data density function  $q(\mathbf{x}_0)$  satisfies a form of Gaussian distribution. The process of recurrent sampling  $\mathbf{x}_{t-1} \sim q(\mathbf{x}_{t-1}|\mathbf{x}_t, \tilde{\mathbf{x}}_0)$  from  $T$  to 0 is equivalent to minimization process of  $D_{KL}[q(\mathbf{x}_0)||p_\theta(\tilde{\mathbf{x}}_0|\mathbf{x}_t)]$  .wrt.  $\mathbf{x}_t$ .

*Proof.* Given real data  $\mathbf{x}_0$ , two latent samples are sampled at two timestep  $t_1 < t_2$ . We have,  $\mathbf{x}_{t_1} = \sqrt{\bar{\alpha}_{t_1}}\mathbf{x}_0 + \sqrt{1 - \bar{\alpha}_{t_1}}\epsilon$  and  $\mathbf{x}_{t_2} = \sqrt{\bar{\alpha}_{t_2}}\mathbf{x}_0 + \sqrt{1 - \bar{\alpha}_{t_2}}\epsilon$ . From  $\mathbf{x}_{t_1}$  and  $\mathbf{x}_{t_2}$ , real data prediction has the form of  $\tilde{\mathbf{x}}_0^{(t_1)} = \frac{\mathbf{x}_{t_1} - \sqrt{1 - \bar{\alpha}_{t_1}}\epsilon_\theta(\mathbf{x}_{t_1}, t_1)}{\sqrt{\bar{\alpha}_{t_1}}}$  and  $\tilde{\mathbf{x}}_0^{(t_2)} = \frac{\mathbf{x}_{t_2} - \sqrt{1 - \bar{\alpha}_{t_2}}\epsilon_\theta(\mathbf{x}_{t_2}, t_2)}{\sqrt{\bar{\alpha}_{t_2}}}$  correspondingly.

Replace  $\mathbf{x}_{t_1}$  and  $\mathbf{x}_{t_2}$  with  $\mathbf{x}_0$  and  $\epsilon$ , we have  $\tilde{\mathbf{x}}_0^{(t_1)} = \mathbf{x}_0 + \frac{\sqrt{1 - \bar{\alpha}_{t_1}}(\epsilon - \epsilon_\theta(\mathbf{x}_{t_1}, t_1))}{\sqrt{\bar{\alpha}_{t_1}}}$  and  $\tilde{\mathbf{x}}_0^{(t_2)} = \mathbf{x}_0 + \frac{\sqrt{1 - \bar{\alpha}_{t_2}}(\epsilon - \epsilon_\theta(\mathbf{x}_{t_2}, t_2))}{\sqrt{\bar{\alpha}_{t_2}}}$ . Thus  $\|\tilde{\mathbf{x}}_0^{(t_1)} - \mathbf{x}_0\| = \frac{1 - \bar{\alpha}_{t_1} \|\epsilon - \epsilon_\theta(\mathbf{x}_{t_1}, t_1)\|}{\bar{\alpha}_{t_1}}$  and  $\|\tilde{\mathbf{x}}_0^{(t_2)} - \mathbf{x}_0\| = \frac{1 - \bar{\alpha}_{t_2} \|\epsilon - \epsilon_\theta(\mathbf{x}_{t_2}, t_2)\|}{\bar{\alpha}_{t_2}}$ . Since  $\epsilon_\theta(\mathbf{x}_{t_1}, t_1) \sim \epsilon_\theta(\mathbf{x}_{t_2}, t_2) \sim \epsilon$ ,  $\|\epsilon - \epsilon_\theta(\mathbf{x}_{t_1}, t_1)\| \approx \|\epsilon - \epsilon_\theta(\mathbf{x}_{t_2}, t_2)\| \approx \Delta$ . This results in  $\|\tilde{\mathbf{x}}_0^{(t_1)} - \mathbf{x}_0\| = \frac{1 - \bar{\alpha}_{t_1}}{\bar{\alpha}_{t_1}} \Delta$  and  $\|\tilde{\mathbf{x}}_0^{(t_2)} - \mathbf{x}_0\| = \frac{1 - \bar{\alpha}_{t_2}}{\bar{\alpha}_{t_2}} \Delta$ .  $\|\tilde{\mathbf{x}}_0^{(t_1)} - \mathbf{x}_0\| < \|\tilde{\mathbf{x}}_0^{(t_2)} - \mathbf{x}_0\|$  since  $\frac{1 - \bar{\alpha}_{t_2}}{\bar{\alpha}_{t_2}} > \frac{1 - \bar{\alpha}_{t_1}}{\bar{\alpha}_{t_1}} \geq 0, \forall t_2 > t_1$ . Consequently, the sampling of  $\mathbf{x}_{t-1} \sim q(\mathbf{x}_{t-1}|\mathbf{x}_t, \tilde{\mathbf{x}}_0)$  from timesteps  $T$  to 0 would mean the minimization of  $\|\tilde{\mathbf{x}}_0^{(t)} - \mathbf{x}_0\|$ . Since  $q(\mathbf{x}_0)$  is a normal distribution, the final objective can be written as  $\min_{\mathbf{x}_t} D_{KL}[q(\mathbf{x}_0)||p_\theta(\tilde{\mathbf{x}}_0|\mathbf{x}_t)]$ . (Full proof can be found in the appendix).  $\square$

If we consider  $\mathbf{x}_t$  of the Eq.8 as the set of optimization parameters, the sampling process will have the objective function:

$$\min_{\mathbf{x}_t} D_{KL}[q(\mathbf{x}_0)||p_\theta(\tilde{\mathbf{x}}_0|\mathbf{x}_t)] \quad (9)$$

We re-write the Eq.8 as:

$$\mathbf{x}_{t-1} = \mathbf{x}_t - \underbrace{\left( \frac{\sqrt{\alpha_t} - 1}{\sqrt{\alpha_t}} \mathbf{x}_t + \frac{1 - \alpha_t}{\sqrt{1 - \bar{\alpha}_t} \sqrt{\alpha_t}} \epsilon_\theta(\mathbf{x}_t, t) - \sigma_t \mathbf{z} \right)}_{\gamma_1 \nabla D_{KL}[q(\mathbf{x}_0)||p_\theta(\tilde{\mathbf{x}}_0|\mathbf{x}_t)]} \quad (10)$$

Eq.10 turns the sampling process into a stochastic gradient descent process where the  $\mathbf{x}_t$  is the parameter of the model at the timestep  $t$ , the updated direction into  $\mathbf{x}_t$  aims to satisfy the objective function Eq.9.

**Classification objective:** From Eq.5, we have the term  $\sigma_t^2 \nabla_{\mathbf{x}_t} \log p_\phi(y|\mathbf{x}_t)$  is added to the sampling equation for guidance. This term can be written in full form as  $\sigma_t^2 \nabla_{\mathbf{x}_t} (q(y) \log q(y) - q(y) \log p_\phi(y|\mathbf{x}_t))$  which is equivalent to  $-\sigma_t^2 \nabla D_{KL}[q(y)||p_\phi(\hat{y}|\mathbf{x}_t)]$ . Combine Eq.10 with guidance information in Eq.5, we have:

$$\mathbf{x}_{t-1} = \mathbf{x}_t - \underbrace{\left( \frac{\sqrt{\alpha_t} - 1}{\sqrt{\alpha_t}} \mathbf{x}_t + \frac{1 - \alpha_t}{\sqrt{1 - \bar{\alpha}_t} \sqrt{\alpha_t}} \epsilon_\theta(\mathbf{x}_t, t) - \sigma_t \mathbf{z} \right)}_{\gamma_1 \nabla D_{KL}[q(\mathbf{x}_0)||p_\theta(\tilde{\mathbf{x}}_0|\mathbf{x}_t)]} - \underbrace{(-\sigma_t^2 \nabla_{\mathbf{x}_t} \log p_\phi(y|\mathbf{x}_t))}_{\gamma_2 \nabla D_{KL}[q(y)||p_\phi(\hat{y}|\mathbf{x}_t)]} \quad (11)$$

As a result, the process of updating  $\mathbf{x}_t$  to  $\mathbf{x}_{t-1}$  is a "training" step to optimize to objective functions  $D_{KL}[q(\mathbf{x}_0)||p_\theta(\tilde{\mathbf{x}}_0|\mathbf{x}_t)]$  and  $D_{KL}[q(y)||p_\phi(\hat{y}|\mathbf{x}_t)]$  with two gradients respecting to  $\mathbf{x}_t$  as Eq.11. Since this is similar to the training process, it is expected to face some problems in training deep neural networks. In this work, the problem of model fitting is detected by observing the losses given by the classification objective during the sampling process.

### 3.1 Model-fitting

Based on the optimization problem from the sampling process in the previous section, we first define *On-sampling loss* and *Off-sampling loss* for observation.

**Definition 1.** *On-sampling loss/accuracy* refers to the loss or accuracy evaluated on the generated samples  $\mathbf{x}_t$  at timestep  $t$  during the diffusion sampling process, which consists of  $T$  timesteps. This loss is obtained by the classifier that provides guidance throughout the sampling process.

**Definition 2.** *Off-sampling loss/accuracy* refers to the loss or accuracy evaluated on the generated samples  $\mathbf{x}_t$  at timestep  $t$  during the diffusion sampling process, which consists of  $T$  timesteps. This loss is obtained by the classifier that **does not** provides guidance throughout the sampling process.

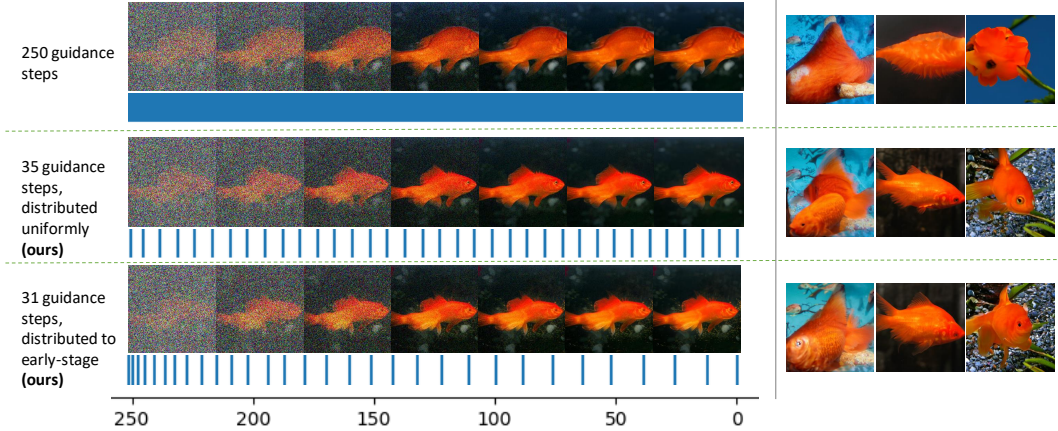


Figure 2: *ImageNet256x256/ADM-G[2]*. The top row is the vanilla guidance, where all the timesteps got the guidance information. The second and third rows are our proposed method, which only applies 35 time steps. The second row distributes the timesteps uniformly, while the third row distributes the timesteps toward the early stage of the sampling process. The Compress Guidance performs significantly better than the original guidance method. One blue stick means one guidance step.

we visualize the *on-sampling* loss obtained from the noise-aware classifier [2] as in Figure 1. We found out that the classification information is only useful during the early stage of the process, as it converges very early in the first 120 timesteps. However, a different trend is observed for the *off-sampling* loss. We set up an off-sampling classifier with the same architecture and performance as the on-sampling classifier used for guidance or in *on-sampling* loss. The only difference between the two models is the parameters. The details on how to obtain this off-sampling classifier are in Appendix... To avoid bias, we also use an off-the-shelf model ResNet152 [7] to be another off-sampling classifier.

**Definition 3.** *Model-fitting* occurs when sampled images  $\mathbf{x}_t$  at timestep  $t$  is updated to maximize  $p_\phi(y|\mathbf{x}_t)$  or to satisfy the parameters of the  $\phi$  only instead of the real distribution  $q(y|\mathbf{x}_t)$ .

In practice, a pretrained  $p_\phi(y|\mathbf{x}_t)$  is only able to capture part of the  $q(y|\mathbf{x}_t)$ . Fitting solely with  $p_\phi(y|\mathbf{x}_t)$  limits the sample’s generalisation ability, leading to incorrect features or overemphasising certain details due to misclassification or overfocusing of the guidance classifier. Three pieces of evidence support that the vanilla guidance suffers from **model-fitting** problem.

**Evidence 1:** From the figures in Table 1, we see that while the on-sampling loss converges around the 120<sup>th</sup> timestep, the off-sampling loss remains high until the diffusion model converges later. This indicates that samples  $\mathbf{x}_t$  at timestep  $t$  satisfy only the on-sampling classifier but not the off-sampling classifier, despite their identical performance and architecture. Although the off-sampling loss decreases by the end, a significant gap between the off-sampling and on-sampling losses persists. This supports our hypothesis that the guidance sampling process produces features that fit only the guidance classifier, not the conditional information.

**Evidence 2:** Table 1 illustrates the model-fitting problem through accuracy metrics. With vanilla guidance, the accuracy is about 90.80% for the on-sampling classifier. However, the same samples evaluated by the off-sampling classifier or Resnet152 achieve only around 62.5% and 34.2% accuracy, respectively. This indicates that many features generated by the model are specific to the guidance classifier and do not generalize to other models.

**Evidence 3:** Figure 2 (first row) shows samples from vanilla guidance, where every sampling step receives guidance information. Applying guidance at all timesteps forces the model to fit the on-sampling classifier’s perception. Often, this makes the model colour-sensitive, focusing on generating the "orange" feature for Goldfish and ignoring other details.

From the three pieces of evidence we can observe, we can conclude that the vanilla guidance scheme has suffered from the model-fitting problem.

**Analogy to overfitting:** In neural network training, we have a dataset  $\mathbf{x}$  and a classifier  $f_\theta(\mathbf{x})$  to approximate the posterior distribution  $p(y|\mathbf{x})$ . Let  $\mathbf{x}_{\text{train}}$  be the training data and  $\mathbf{x}_{\text{test}}$  the testing data. Overfitting occurs when  $f_\theta$  is tailored to fit  $\mathbf{x}_{\text{train}}$  but fails to generalize to the entire dataset  $\mathbf{x}$ . This is observed by the gap between training loss/accuracy and testing loss/accuracy on  $\mathbf{x}_{\text{train}}$  and  $\mathbf{x}_{\text{test}}$ .

Table 1: Evaluation on ImageNet64x64 sampled by ADM-G [2]. There exists a significant gap between the on-sampling and the off-sampling classifier in terms of accuracy and loss.

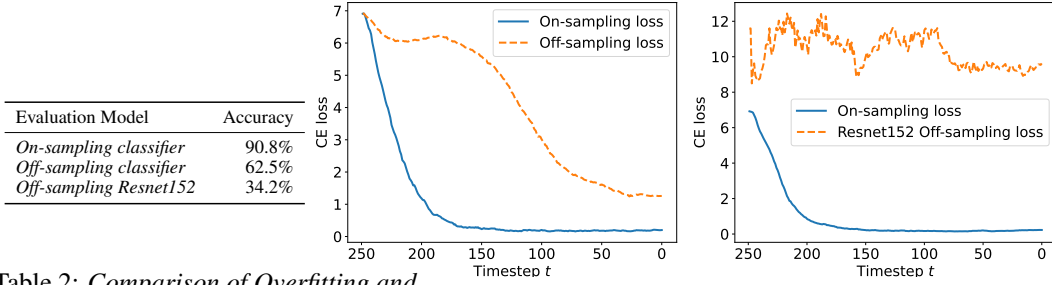


Table 2: Comparison of Overfitting and Model-Fitting

Aspect	Overfitting	Model-fitting
Train Data	$\mathbf{x}_{\text{train}}$	$f_{\phi_g}$
Test Data	$\mathbf{x}_{\text{test}}$	$f_{\phi_o}$
Parameters	$f_{\phi}$	$\mathbf{x}$

In the diffusion model’s sampling process, the classifier  $f_{\theta}$  is pretrained or fixed. The aim is to adjust the samples  $\mathbf{x}$  to match the trained posterior  $p_{\theta}(y|\mathbf{x})$ . This process also uses Stochastic Gradient Descent with different roles:  $f_{\phi_g}$  acts as the fixed data, and  $\mathbf{x}$  are the trainable parameters. The model-fitting problem arises when  $\mathbf{x}$  is adjusted to fit

only the specific  $f_{\theta}$  instead of generalizing well. Here,  $f_{\phi_g}$  is the on-sampling "data", and we use an off-sampling "data"  $f_{\phi_o}$  to observe the model-fitting where the gap between them is large, analogous to using training and testing data to check for overfitting.

### 3.2 Compress Guidance

From Figure 1, we have already shown that the guidance loss is mainly active from 250<sup>th</sup> to 200<sup>th</sup> timestep. Doing guidance further might result in harmful features in the generated samples. Thus, reducing guidance timesteps is an economical and effective method to help us achieve a good sampling process. The question is, how do we reduce the guidance steps?

We propose a simple approach to solve the overfitting problem. Start with the sampling Eq.11; we denote the number of timesteps that we want to do guidance is  $l$ , and the set  $G$  is the set of timesteps that guidance will be applied. The sampling process can be modified as below:

$$\mathbf{x}_{t-1} = \begin{cases} \mathbf{x}_t - \gamma_1 \nabla D_{KL}[q(\tilde{\mathbf{x}}_0|\mathbf{x}_t)||q(\mathbf{x}_0)] - \gamma_2 \nabla D_{KL}[q(\hat{y}|\mathbf{x}_t)||q(y)], & \text{if } t \in G \\ \mathbf{x}_t - \gamma_1 \nabla D_{KL}[q(\tilde{\mathbf{x}}_0|\mathbf{x}_t)||q(\mathbf{x}_0)], & \text{otherwise} \end{cases} \quad (12)$$

The intuition is that guidance is more important toward the early stage of the sampling process. Thus, we propose a method that distributes more guidance toward the early sampling stage as Eq.13.

$$G_i = T - \lfloor \frac{T}{|G|^k} i^k \rfloor \quad \forall 0 \leq i \leq l, k \in [0; +\infty] \quad (13)$$

**Theorem 2.** When  $k \rightarrow +\infty$ , the guidance timesteps will be distributed more toward the early stage of the sampling process.

**Theorem 3.** When  $k < 1$  and  $k \rightarrow 0$ , the guidance timesteps will be distributed more toward the late stage of the sampling process.

The proposed solution to select the timesteps for guidance as Eq.13 allows us to choose the number of timesteps we will do guidance and how to distribute these timesteps along the sampling process by adjusting the  $k$  values. The full proof of Theorem 2 and 3 is written in the appendix.

## 4 Experimental results

**Setup** Experiments are conducted on pretrained Diffusion models on *ImageNet 64x64*, *ImageNet 128x128*, *ImageNet 256x256* and *MSCOCO*. The base Diffusion models utilized for label condition sampling task are ADM [2] and CADM [2] for classifier guidance, DiT[8] for classifier-free guidance (CFG) [1], GLIDE[9] for CLIP text-to-image guidance and Stable Diffusion [10] for text-to-image classifier-free guidance. Other baselines we also do comparison is BigGAN [11], VAQ-VAE-2 [12], LOGAN [13], DCTransformers [14]. FID/sFID, Precision and Recall are utilized to evaluate image



Figure 3: *Qualitative results on ImageNet256x256. Left: Vanilla guidance applied at all timesteps. Right: Compress Guidance applied at 50 out of 250 timesteps. Compress Guidance reduces over-emphasized features, correcting weird and incorrect details. Further results are in AppendixH*



Figure 4: *Qualitative results on ImageNet256x256. Left: Vanilla guidance applied at all timesteps. Right: Compress Guidance applied at 50 of 250 timesteps. Compress Guidance corrects misclassification by the on-sampling classifier, preventing out-of-class image generation and restoring accurate class information. More qualitative results are shown in AppendixH*

quality and diversity measurements. We denote Compress Guidance as "-CompG" and "-G" as vanilla guidance, "-CFG" is the CFG, and "-CompCFG" is our proposed Compress Guidance applying on CFG. Full results with details of the experimental set up are discussed in Appendix C and D.

#### 4.1 Classifier Guidance

For classifier guidance, we distinguish this guidance scheme into two types due to its behaviour discrepancy when applying the guidance. The first type is classifier guidance on the unconditional diffusion model, and the second is classifier guidance on the conditional diffusion model.

**Guidance with unconditional diffusion model** Guidance with unconditional model provides diffusion model both conditional information and image quality improvement [2]. Table 3 shows the improvement using Compress Guidance (CompG). The results show three main improvements. First, there is an improvement in the quantitative results of FID, sFID, and Recall values, indicating an improvement in generated image qualities and diversity. Second, we further validate the image quality and diversity improvement in Figure 3 and 4. Third, the proposed method offered a significant improvement in running time where we reduced the number of guidance steps by 5 times and reduced the running time by 42% on ImageNet64x64 and 23% on ImageNet256x256.

**Guidance with conditional diffusion model** Unlike the unconditional diffusion model, guidance in the conditional diffusion model does not aim to provide conditional information. Therefore, the effect of guidance is less significant than guidance on the unconditional diffusion model. Table 4 shows the diversity improvement based on Recall values compared to vanilla guidance. Furthermore, CompG reduced the guidance steps by 5 times and reduced the sampling time by 39.79% , 29.63% , and 22% on ImageNet64x64, 128x128 and 256x256, respectively.

Table 3: Applying CompG over ADM-G reduces the number of guidance timesteps by fivefold and increases the sampling process’s running time by approximately 42% on ImageNet64x64 and 23% on ImageNet256x256. Notably, on ImageNet256x256, the running time of ADM-CompG is only 5% higher compared to the unguided sampling process. In terms of performance, ADM-CompG significantly outperforms ADM and ADM-G across most metrics.

Model	$ G $ ( $\downarrow$ )	GPU hours ( $\downarrow$ )	FID ( $\downarrow$ )	sFID ( $\downarrow$ )	Prec ( $\uparrow$ )	Rec ( $\uparrow$ )
<b>ImageNet 64x64</b>						
ADM (No guidance)	0	26.33	9.95	6.58	0.60	0.65
ADM-G	250	54.86	6.40	9.67	<b>0.73</b>	0.54
<b>ADM-CompG</b>	<b>50</b>	<b>31.80</b>	<b>5.91</b>	<b>8.26</b>	0.71	<b>0.56</b>
<b>ImageNet 256x256</b>						
ADM (No guidance)	0	245.37	26.21	6.35	0.61	0.63
ADM-G	250	334.25	11.96	10.28	0.75	0.45
<b>ADM-CompG</b>	<b>50</b>	<b>258.33</b>	<b>11.65</b>	<b>8.52</b>	<b>0.75</b>	<b>0.48</b>

Table 4: Applying CompG to classifier guidance in conditional diffusion models and classifier-free guidance significantly improves performance. CADM-CompG outperforms CADM and slightly surpasses CADM-G, as CADM-G depends on both the classifier and conditional diffusion model. CompG reduces the number of guidance timesteps by fivefold and significantly increases the sampling process’s running time across all three ImageNet resolutions. CompG for classifier-free guidance also reduces the number of guidance steps by tenfold and achieves significantly better results.

Model	$ G $ ( $\downarrow$ )	GPU hours ( $\downarrow$ )	FID ( $\downarrow$ )	sFID ( $\downarrow$ )	Prec ( $\uparrow$ )	Rec ( $\uparrow$ )
<b>ImageNet 64x64</b>						
CADM (No guidance)	0	26.64	2.07	4.29	0.73	0.63
CADM-G	250	53.52	2.47	4.88	<b>0.80</b>	0.57
<b>CADM-CompG</b>	<b>50</b>	<b>32.22</b>	<b>1.91</b>	<b>4.57</b>	0.77	<b>0.61</b>
CADM-CFG	250	54.97	1.89	4.45	<b>0.77</b>	0.60
<b>CADM-CompCFG</b>	<b>25</b>	<b>29.29</b>	<b>1.84</b>	<b>4.38</b>	<b>0.77</b>	<b>0.61</b>
<b>ImageNet 128x128</b>						
CADM (No guidance)	0	61.60	6.14	4.96	0.69	0.65
CADM-G	250	94.06	2.95	5.45	<b>0.81</b>	0.54
<b>CADM-CompG</b>	<b>50</b>	<b>66.19</b>	<b>2.86</b>	<b>5.29</b>	0.79	<b>0.58</b>
<b>ImageNet 256x256</b>						
CADM (No guidance)	0	240.33	10.94	6.02	0.69	0.63
CADM-G	250	336.05	4.58	<b>5.21</b>	0.81	0.51
<b>CADM-CompG</b>	<b>50</b>	<b>259.25</b>	<b>4.52</b>	5.29	<b>0.82</b>	<b>0.51</b>
DiT-CFG	250	75.04	2.25	<b>4.56</b>	0.82	0.58
<b>DiT-CompCFG</b>	<b>22</b>	<b>42.20</b>	<b>2.19</b>	4.74	<b>0.82</b>	<b>0.60</b>

## 4.2 Classifier-free guidance

Classifier-free guidance is a different form of guidance from classifier guidance. Although classifier-free guidance does not use an explicit classifier for guidance, the diffusion model serves as an implicit classifier inside the model as discussed in Appendix F. We hypothesize that classifier-free guidance also suffers from a similar problem with classifier guidance. We apply the Compress Guidance technique on classifier-free guidance (CompCFG) and demonstrate the results in Table 4.

## 4.3 Text-to-Image Guidance

Besides using labels for conditional generation, text-to-image allows users to input text conditions and generate images with similar meanings. This task has recently become one of the most popular tasks in generative models. We apply the Compress Guidance on this task with two types of guidances, which are CLIP-based guidance (GLIDE) [9] and classifier-free guidance (Stable Diffusion) [10]. The results are shown in Table 5 and 6 and qualitatively show in Figure 1.



Table 5: *GLIDE* [9] is a Text-to-image model with classifier-based guidance. We evaluate the *GLIDE* performance on MSCoco64x64 and MSCoco256x256.

Model	$ G $ ( $\downarrow$ )	GPU hours ( $\downarrow$ )	Zeroshot FID ( $\downarrow$ )
<b>MSCOCO 64x64</b>			
GLIDE-G	250	34.04	24.78
<b>GLIDE-CompG</b>	<b>25</b>	<b>20.93</b>	<b>24.5</b>
<b>MSCOCO 256x256</b>			
GLIDE-G	250	66.84	34.78
<b>GLIDE-CompG</b>	<b>35</b>	<b>37.55</b>	<b>33.12</b>

Table 6: *Stable Diffusion* is one of the models that inherit the success of applying classifier-free guidance. We apply the Compress Guidance technique with *Stable Diffusion* with classifier-free guidance and obtain significant improvement in both qualitative results as in Figure 1 and quantitative results as below.

Model	$ G $ ( $\downarrow$ )	GPU hours ( $\downarrow$ )	FID ( $\downarrow$ )	IS ( $\uparrow$ )
<b>MSCOCO 256x256</b>				
SD-CFG	50	54	16.04	32.34
<b>SD-ComptCFG</b>	<b>8</b>	<b>35</b>	<b>14.04</b>	<b>35.90</b>

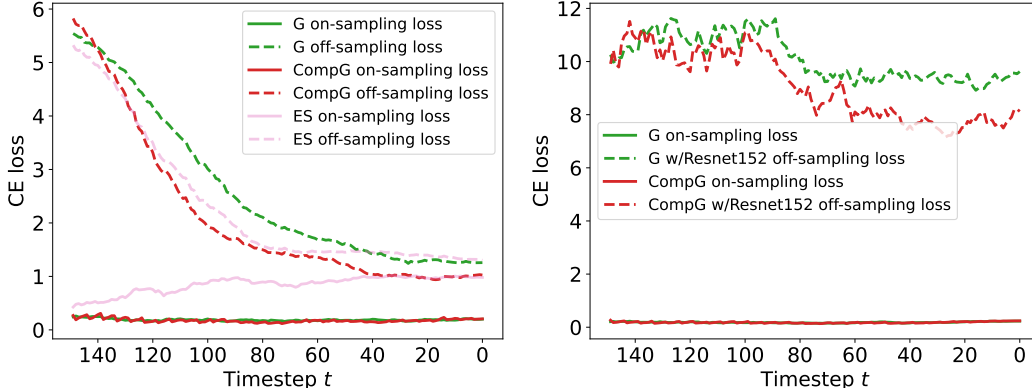


Figure 5: *CompG* reduces the gap between off-sampling and on-sampling loss, mitigating the model-fitting issue compared to other schemes. The *ES* scheme concludes guidance after 50 steps and suffers from forgetting problems where the on-sampling loss increases along with the sampling process. Visualization starts from timestep 150 due to the noticeable divergence in lines thereafter.

#### 4.4 Ablation study

Table 7: Evaluation on *ImageNet64x64* samples. *ES* suffers from forgetting problem and has low performance. *CompG* achieves higher both on on-sampling and oof-sampling acc.

Guidance	On-samp.	Off-samp.	Resnet
Vanilla	90.8	62.5	34.17
Early Stopping	63.05	55.22	33.55
<b>CompG (ours)</b>	<b>91.2</b>	<b>64.2</b>	<b>34.93</b>

**Solving the model-fitting problem** One of the main contributions of the proposed method is its help in alleviating the model-fitting problem. Due to the closeness between the model-fitting problem and overfitting problems, we use an Early stopping scheme for comparison. For *CompG*, we utilize 50 guidance steps. Thus, we also turn off guidance for the *ES* scheme after 50 guidance calls. Figure 5 for details.

**Distribution guidance timesteps toward the early stage of the process:** According to the Theorem 2, by adjusting  $k$ , we can distribute the timesteps toward the early stage or the late stage of the sampling process. Table 8 shows the comparison between  $k$  values. With  $k = 1.0$ , guidance steps are distributed uniformly and achieve the best results. However, larger  $k$  results in poorer performance but more fruitful running time and number of guidance steps.

Table 8: *ImageNet64x64*. Experimental results with increasing  $k$ . According to Theorem 2, increasing  $k$  guides distribution towards early timesteps, resulting in worsened performance comparable to full guidance. However, fewer guidance steps lead to significantly lower running costs with large  $k$ .

Model	k	$ G $ ( $\downarrow$ )	GPU hours ( $\downarrow$ )	FID ( $\downarrow$ )	sFID ( $\downarrow$ )	Prec ( $\uparrow$ )	Rec ( $\uparrow$ )
CADM (No guidance)	-	0	26.64	2.07	4.29	0.73	0.63
CADM-ComptG	1.0	25	29.29	<b>1.84</b>	<b>4.38</b>	<b>0.77</b>	<b>0.61</b>
CADM-ComptG	1.3	19	28.65	1.91	4.58	0.76	0.61
CADM-ComptG	1.5	16	28.16	1.92	4.68	0.76	0.61
CADM-ComptG	2.0	<b>13</b>	<b>27.94</b>	1.93	4.74	0.76	0.62

**Trade-off between computation and image quality** Compact rate is the total number of sampling steps over the number of guidance steps  $\frac{T}{|G|}$ . The larger the compact rate, the lower the model's

guidance, hence the lower running time. Figure 6 shows the effect of using fewer timesteps on IS, FID and Recall as in Figure 6a, 6b and 6c in Appendix.

## 5 Conclusion

The paper quantifies the problem of model-fitting, an analogy to the problem of overfitting in training deep neural networks by observing on-sampling loss and off-sampling loss. Compress Guidance is proposed to alleviate the problem and significantly boost the Diffusion Model’s performance in terms of both qualitative and quantitative results. Furthermore, applying Compress Guidance can reduce the number of guidance steps by at least 5 times and reduce the running time by around 40%. Limitations/Broader Impacts and Safeguards will be discussed in the Appendix.

## References

- [1] Jonathan Ho and Tim Salimans. Classifier-free diffusion guidance. *arXiv preprint arXiv:2207.12598*, 2022.
- [2] Prafulla Dhariwal and Alexander Nichol. Diffusion models beat gans on image synthesis. *Advances in neural information processing systems*, 34:8780–8794, 2021.
- [3] Arpit Bansal, Hong-Min Chu, Avi Schwarzschild, Soumyadip Sengupta, Micah Goldblum, Jonas Geiping, and Tom Goldstein. Universal guidance for diffusion models. In *Proceedings of the IEEE/CVF Conference on Computer Vision and Pattern Recognition*, pages 843–852, 2023.
- [4] Xihui Liu, Dong Huk Park, Samaneh Azadi, Gong Zhang, Arman Chopikyan, Yuxiao Hu, Humphrey Shi, Anna Rohrbach, and Trevor Darrell. More control for free! image synthesis with semantic diffusion guidance. In *Proceedings of the IEEE/CVF Winter Conference on Applications of Computer Vision*, pages 289–299, 2023.
- [5] Dave Epstein, Allan Jabri, Ben Poole, Alexei Efros, and Aleksander Holynski. Diffusion self-guidance for controllable image generation. *Advances in Neural Information Processing Systems*, 36:16222–16239, 2023.
- [6] Jonathan Ho, Ajay Jain, and Pieter Abbeel. Denoising diffusion probabilistic models. *Advances in neural information processing systems*, 33:6840–6851, 2020.
- [7] Kaiming He, Xiangyu Zhang, Shaoqing Ren, and Jian Sun. Deep residual learning for image recognition, 2015.
- [8] William Peebles and Saining Xie. Scalable diffusion models with transformers. In *Proceedings of the IEEE/CVF International Conference on Computer Vision*, pages 4195–4205, 2023.
- [9] Alex Nichol, Prafulla Dhariwal, Aditya Ramesh, Pranav Shyam, Pamela Mishkin, Bob McGrew, Ilya Sutskever, and Mark Chen. Glide: Towards photorealistic image generation and editing with text-guided diffusion models. *arXiv preprint arXiv:2112.10741*, 2021.
- [10] Robin Rombach, Andreas Blattmann, Dominik Lorenz, Patrick Esser, and Björn Ommer. High-resolution image synthesis with latent diffusion models. In *Proceedings of the IEEE/CVF conference on computer vision and pattern recognition*, pages 10684–10695, 2022.
- [11] Andrew Brock, Jeff Donahue, and Karen Simonyan. Large scale gan training for high fidelity natural image synthesis. *arXiv preprint arXiv:1809.11096*, 2018.
- [12] Yang Zhao, Chunyuan Li, Ping Yu, Jianfeng Gao, and Changyou Chen. Feature quantization improves gan training. *arXiv preprint arXiv:2004.02088*, 2020.
- [13] Yan Wu, Jeff Donahue, David Balduzzi, Karen Simonyan, and Timothy Lillicrap. Logan: Latent optimisation for generative adversarial networks. *arXiv preprint arXiv:1912.00953*, 2019.
- [14] Charlie Nash, Jacob Menick, Sander Dieleman, and Peter W Battaglia. Generating images with sparse representations. *arXiv preprint arXiv:2103.03841*, 2021.
- [15] Anh-Dung Dinh, Daochang Liu, and Chang Xu. Pixelasparam: A gradient view on diffusion sampling with guidance. In *International Conference on Machine Learning*, pages 8120–8137. PMLR, 2023.

- [16] Yang Song, Jascha Sohl-Dickstein, Diederik P Kingma, Abhishek Kumar, Stefano Ermon, and Ben Poole. Score-based generative modeling through stochastic differential equations. *arXiv preprint arXiv:2011.13456*, 2020.
- [17] Arash Vahdat, Karsten Kreis, and Jan Kautz. Score-based generative modeling in latent space. *Advances in neural information processing systems*, 34:11287–11302, 2021.
- [18] Yang Song and Stefano Ermon. Improved techniques for training score-based generative models. *Advances in neural information processing systems*, 33:12438–12448, 2020.
- [19] Bahjat Kawar, Shiran Zada, Oran Lang, Omer Tov, Huiwen Chang, Tali Dekel, Inbar Mosseri, and Michal Irani. Imagic: Text-based real image editing with diffusion models. In *Proceedings of the IEEE/CVF Conference on Computer Vision and Pattern Recognition*, pages 6007–6017, 2023.
- [20] Yi Huang, Jiancheng Huang, Yifan Liu, Mingfu Yan, Jiayi Lv, Jianzhuang Liu, Wei Xiong, He Zhang, Shifeng Chen, and Liangliang Cao. Diffusion model-based image editing: A survey, 2024.
- [21] Jiaming Song, Chenlin Meng, and Stefano Ermon. Denoising diffusion implicit models. *arXiv preprint arXiv:2010.02502*, 2020.
- [22] Qinsheng Zhang and Yongxin Chen. Fast sampling of diffusion models with exponential integrator. *arXiv preprint arXiv:2204.13902*, 2022.
- [23] Tim Salimans and Jonathan Ho. Progressive distillation for fast sampling of diffusion models. *arXiv preprint arXiv:2202.00512*, 2022.
- [24] Axel Sauer, Dominik Lorenz, Andreas Blattmann, and Robin Rombach. Adversarial diffusion distillation. *arXiv preprint arXiv:2311.17042*, 2023.
- [25] Yanyu Li, Huan Wang, Qing Jin, Ju Hu, Pavlo Chemerys, Yun Fu, Yanzhi Wang, Sergey Tulyakov, and Jian Ren. Snapfusion: Text-to-image diffusion model on mobile devices within two seconds. *Advances in Neural Information Processing Systems*, 36, 2024.

## A Limitations of the work

Although the work has performed well in terms of both qualitative, quantitative, and efficiency, it faces a serious problem in selecting hyperparameters. Depending on whether the task requires fast sampling or slow sampling but a good-quality image, we can choose the different values of  $|G|$ . After choosing  $|G|$ , the value of scale guidance needs to be selected carefully since a different  $|G|$  value is associated with a totally different scale guidance to obtain the point that it can generate good-quality images. Further than that, we have hyperparameter  $k$ , which is responsible for moving the guidance toward the start of the sampling or the end of the sampling process is another factor. It significantly helps to reduce  $|G|$ , yet it requires tuning to see the performance trend to select the best  $|G|$  and guidance scale. Future work will try to alleviate the dependence on the hyperparameter selection.

## B Broader impact and safeguard

The work does not have concerns about safeguarding since it does not utilize the training data. The paper only utilizes the pre-trained models from DiT [8], ADM[2], GLIDE [9] and Stable Diffusion [10]. The work fastens the sampling process of the diffusion model and contributes to the population of the diffusion model in reality. However, the negative impact might be on the research on a generative model where bad people use that to fake videos or images.

## C Experimental setup

**Off-sampling classifier:** Off-sampling classifier is initialized as the parameters of the on-sampling classifier. We fine-tune the model with 10000 timesteps with the same loss for training on-sampling classifier. The testing accuracy between off-sampling classifier and on-sampling classifier is shown in Table 9

Evaluation Model	Accuracy
<i>On-sampling classifier</i>	64.5%
<i>Off-sampling classifier</i>	63.5%

Table 9: Testing accuracy between On-sampling classifier and Off-sampling classifier

Figure 11 shows all the hyperparameters used for all experiments in the paper. Normally, since we skip a lot of time steps that provide guidance, the process will fall into the category of forgetting. To avoid this situation, we would increase the guidance scale significantly. The value of the guidance scale is often based on the compact rate  $\frac{T}{|G|}$ . A more significant compact rate also indicates a larger guidance scale.

In Table 7 and Figure 5, to achieve a fair comparison, we tune the guidance scale of CompG to achieve a similar Recall value with vanilla guidance. The reason is that the higher the level of diversity, the harder features can be recognized, resulting in higher loss and lower accuracy. If we don't configure similar diversity between the two schemes, the one with higher diversity will always achieve lower accuracy and higher loss value. We want to avoid the case that the model only samples one good image for all.

For all the tables, the models which are in bold are the proposed.

**GPU hours:** All the GPU hours are calculated based on the time for sampling 50000 samples in ImageNet or 30000 samples in MSCoco.

All experiments are run on a cluster with 4 V100 GPUs.

## D Full comparison

Table 10 shows full comparison with different famous baselines.

## E Mathematical details

### Proof of Theorem 1

*Proof.* Given real data  $\mathbf{x}_0$ , we sample two latent samples at two timestep  $t_1 < t_2$ . As a result  $\mathbf{x}_{t_1} = \sqrt{\bar{\alpha}_{t_1}}\mathbf{x}_0 + \sqrt{1 - \bar{\alpha}_{t_1}}\epsilon$  and  $\mathbf{x}_{t_2} = \sqrt{\bar{\alpha}_{t_2}}\mathbf{x}_0 + \sqrt{1 - \bar{\alpha}_{t_2}}\epsilon$ . From  $\mathbf{x}_{t_1}$  and  $\mathbf{x}_{t_2}$ , the prediction of real data has

Table 10: We show full results of the model compare to other models not related to guidance.

Model	$ G $ ( $\downarrow$ )	GPU hours ( $\downarrow$ )	FID ( $\downarrow$ )	sFID ( $\downarrow$ )	Prec ( $\uparrow$ )	Rec ( $\uparrow$ )
<b>ImageNet 64x64</b>						
BigGAN	-	-	4.06	3.96	0.79	0.48
IDDPM	0	28.32	2.90	3.78	0.73	0.62
CADM (No guidance)	0	26.64	2.07	4.29	0.73	0.63
CADM-G	250	53.52	2.47	4.88	<b>0.80</b>	0.57
<b>CADM-CompG</b>	<b>50</b>	<b>32.22</b>	<b>1.91</b>	<b>4.57</b>	0.77	<b>0.61</b>
CADM-CFG	250	54.97	1.89	4.45	<b>0.77</b>	0.60
<b>CADM-CompCFG</b>	<b>25</b>	<b>29.29</b>	<b>1.84</b>	<b>4.38</b>	<b>0.77</b>	<b>0.61</b>
<b>ImageNet 128x128</b>						
BigGAN	-	-	6.02	7.18	0.86	0.35
LOGAN	-	-	3.36	-	-	-
CADM (No guidance)	0	61.60	6.14	4.96	0.69	0.65
CADM-G	250	94.06	2.95	5.45	<b>0.81</b>	0.54
<b>CADM-CompG</b>	<b>50</b>	<b>66.19</b>	<b>2.86</b>	<b>5.29</b>	0.79	<b>0.58</b>
<b>ImageNet 256x256</b>						
BigGAN	-	-	7.03	7.29	0.87	0.27
DCTrans	-	-	36.51	8.24	0.36	0.67
VQ-VAE-2	-	-	31.11	17.38	0.36	0.57
IDDPM	-	-	12.26	5.42	0.70	0.62
CADM (No guidance)	0	240.33	10.94	6.02	0.69	0.63
CADM-G	250	336.05	4.58	<b>5.21</b>	0.81	0.51
<b>CADM-CompG</b>	<b>50</b>	<b>259.25</b>	<b>4.52</b>	5.29	<b>0.82</b>	<b>0.51</b>
DiT-CFG	250	75.04	2.25	<b>4.56</b>	0.82	0.58
<b>DiT-CompCFG</b>	<b>22</b>	<b>42.20</b>	<b>2.19</b>	4.74	<b>0.82</b>	<b>0.60</b>

the form of  $\tilde{\mathbf{x}}_0^{(t_1)} = \frac{\mathbf{x}_{t_1} - \sqrt{1 - \bar{\alpha}_{t_1}} \epsilon_\theta(\mathbf{x}_{t_1}, t_1)}{\sqrt{\bar{\alpha}_{t_1}}}$  and  $\tilde{\mathbf{x}}_0^{(t_2)} = \frac{\mathbf{x}_{t_2} - \sqrt{1 - \bar{\alpha}_{t_2}} \epsilon_\theta(\mathbf{x}_{t_2}, t_2)}{\sqrt{\bar{\alpha}_{t_2}}}$  correspondingly. Replace  $\mathbf{x}_{t_1}$  and  $\mathbf{x}_{t_2}$  with  $\mathbf{x}_0$  and  $\epsilon$ , we have  $\tilde{\mathbf{x}}_0^{(t_1)} = \mathbf{x}_0 + \frac{\sqrt{1 - \bar{\alpha}_{t_1}} (\epsilon - \epsilon_\theta(\mathbf{x}_{t_1}, t_1))}{\sqrt{\bar{\alpha}_{t_1}}}$  and  $\tilde{\mathbf{x}}_0^{(t_2)} = \mathbf{x}_0 + \frac{\sqrt{1 - \bar{\alpha}_{t_2}} (\epsilon - \epsilon_\theta(\mathbf{x}_{t_2}, t_2))}{\sqrt{\bar{\alpha}_{t_2}}}$ . Thus  $\|\tilde{\mathbf{x}}_0^{(t_1)} - \mathbf{x}_0\| = \frac{1 - \bar{\alpha}_{t_1} \|\epsilon - \epsilon_\theta(\mathbf{x}_{t_1}, t_1)\|}{\bar{\alpha}_{t_1}}$  and  $\|\tilde{\mathbf{x}}_0^{(t_2)} - \mathbf{x}_0\| = \frac{1 - \bar{\alpha}_{t_2} \|\epsilon - \epsilon_\theta(\mathbf{x}_{t_2}, t_2)\|}{\bar{\alpha}_{t_2}}$ . Since  $\epsilon_\theta(\mathbf{x}_{t_1}, t_1) \sim \epsilon_\theta(\mathbf{x}_{t_2}, t_2) \sim \epsilon$ ,  $\|\epsilon - \epsilon_\theta(\mathbf{x}_{t_1}, t_1)\| \approx \|\epsilon - \epsilon_\theta(\mathbf{x}_{t_2}, t_2)\| \approx \Delta$ . This results in  $\|\tilde{\mathbf{x}}_0^{(t_1)} - \mathbf{x}_0\| = \frac{1 - \bar{\alpha}_{t_1}}{\bar{\alpha}_{t_1}} \Delta$  and  $\|\tilde{\mathbf{x}}_0^{(t_2)} - \mathbf{x}_0\| = \frac{1 - \bar{\alpha}_{t_2}}{\bar{\alpha}_{t_2}} \Delta$ .  $\|\tilde{\mathbf{x}}_0^{(t_1)} - \mathbf{x}_0\| < \|\tilde{\mathbf{x}}_0^{(t_2)} - \mathbf{x}_0\|$  since  $\frac{1 - \bar{\alpha}_{t_2}}{\bar{\alpha}_{t_2}} > \frac{1 - \bar{\alpha}_{t_1}}{\bar{\alpha}_{t_1}} \geq 0, \forall t_2 > t_1$ . As a result, the sampling of  $\mathbf{x}_{t-1} \sim q(\mathbf{x}_{t-1} | \mathbf{x}_t, \tilde{\mathbf{x}}_0)$  from timesteps  $T$  to 0 would result in the minimization of  $\|\tilde{\mathbf{x}}_0^{(t)} - \mathbf{x}_0\|$ . Since  $q(\mathbf{x}_0)$  has the form of Gaussian, we can have the minimization of  $\|\tilde{\mathbf{x}}_0^{(t)} - \mathbf{x}_0\|$  would result in the minimization of  $\|q(\tilde{\mathbf{x}}_0) - q(\mathbf{x}_0)\| = \left\| \frac{q(\tilde{\mathbf{x}}_0)q(\mathbf{x}_t | \tilde{\mathbf{x}}_0)}{q(\mathbf{x}_t)} - q(\mathbf{x}_0) \right\|$  since  $\tilde{\mathbf{x}}_0 \sim p_\theta(\tilde{\mathbf{x}}_0 | \mathbf{x}_t)$  with a deterministic forward of  $\mathbf{x}_t$  to  $\epsilon_\theta$ , we have  $q(\tilde{\mathbf{x}}_0) \approx \frac{q(\tilde{\mathbf{x}}_0)q(\mathbf{x}_t | \tilde{\mathbf{x}}_0)}{q(\mathbf{x}_t)} = p_\theta(\tilde{\mathbf{x}}_0 | \mathbf{x}_t)$ .

Assume we have two density function  $p(\mathbf{x})$  and  $q(\mathbf{x})$ . The KL divergence between these two has the form:

$$\int_0^1 p(\mathbf{x}) \log \frac{p(\mathbf{x})}{q(\mathbf{x})} = \int_0^1 p(\mathbf{x}) \log(p(\mathbf{x})) - p(\mathbf{x}) \log(q(\mathbf{x})) d\mathbf{x} \quad (14)$$

$$= \int_0^1 p(\mathbf{x}) \log(p(\mathbf{x})) d\mathbf{x} - \int_0^1 p(\mathbf{x}) \log(p(\mathbf{x})) + p(\mathbf{x}) \log\left(\frac{p(\mathbf{x})}{q(\mathbf{x})} - 1\right) + 1 d\mathbf{x} \quad (15)$$

$$= \int_0^1 -p(\mathbf{x}) \log\left(\frac{q(\mathbf{x})}{p(\mathbf{x})} - 1\right) + 1 d\mathbf{x} \quad (16)$$

$$= \int_0^1 -(q(\mathbf{x}) - p(\mathbf{x})) + (q(\mathbf{x}) - p(\mathbf{x}))^2 \left(\frac{1}{p(\mathbf{x})} - \frac{1}{q(\mathbf{x})}\right) d\mathbf{x} \quad (17)$$

$$\leq \int_0^1 (q(\mathbf{x}) - p(\mathbf{x}))^2 \left(\frac{1}{p(\mathbf{x})} - \frac{1}{q(\mathbf{x})}\right) d\mathbf{x} \quad (18)$$

$$\leq \int_0^1 (q(\mathbf{x}) - p(\mathbf{x}))^2 \left(\frac{1}{a} - \frac{1}{b}\right) d\mathbf{x} = \frac{b-a}{ab} \|p - q\| \quad (19)$$

Thus  $D_{KL}(p(\mathbf{x}) || q(\mathbf{x})) \leq \frac{b-a}{ab} \|p - q\|$

Base on this bound we would have the minimization of  $\|p_\theta(\tilde{\mathbf{x}}_0|\mathbf{x}_t) - q(\mathbf{x}_0)\|$  is equivalent to the minimization of  $D_{KL}(q(\mathbf{x}_0)||p_\theta(\tilde{\mathbf{x}}_0|\mathbf{x}_t))$ .  $\square$

### Proof of Theorem 2

*Proof.* Let  $k_1 < k_2$  and  $k_1, k_2 \in [1; +\infty]$ , with  $\frac{T}{|G|^k} i^k = T(\frac{i}{|G|})^k$  and  $\frac{i}{|G|} < 1$ , we have:

$$\left(\frac{i}{|G|}\right)^{k_1} \geq \left(\frac{i}{|G|}\right)^{k_2} \quad (20)$$

$$\Leftrightarrow T\left(\frac{i}{|G|}\right)^{k_1} \geq T\left(\frac{i}{|G|}\right)^{k_2} \quad (21)$$

$$\Leftrightarrow \lfloor T\left(\frac{i}{|G|}\right)^{k_1} \rfloor \geq \lfloor T\left(\frac{i}{|G|}\right)^{k_2} \rfloor \quad (22)$$

$$\Leftrightarrow T - \lfloor T\left(\frac{i}{|G|}\right)^{k_1} \rfloor \leq T - \lfloor T\left(\frac{i}{|G|}\right)^{k_2} \rfloor \quad (23)$$

As a result,  $G_i^{(k_1)} \leq G_i^{(k_2)} \forall k_1, k_2 \geq 1$  and  $k_1 < k_2$ . With  $k_2 \rightarrow +\infty$ ,  $G_i^{(k_2)}$  is bounded by T. This means that larger  $k$  values would result in the distribution of the timesteps toward the early stage of the sampling process.  $\square$

### Proof of Theorem 3

*Proof.* Similar to previous proof we have  $G_i^{(k_1)} \leq G_i^{(k_2)} \forall k_1, k_2 \geq 1$  and  $k_1 < k_2$ . This also mean that  $G_i^{(k_1)} > G_i^{(1)}$ ,  $\forall 0 \leq k_1 < 1$  and if  $k_1 \rightarrow 0$  then  $G_i^{(k_1)} \rightarrow 0$ , hence all the  $g_i \in G^{(k_1)_i}$  is bounded by 0. As a result, by adjusting  $k$  toward 0, we would have the distribution of guidance steps toward the later stage of the sampling process  $\square$

## F CompG and classifier-free guidance

We start from the noise sampling equation of the classifier-free guidance as:

$$\tilde{\epsilon} = (1 + w)\epsilon_\theta(\mathbf{x}_t, c, t) - w\epsilon_\theta(\mathbf{x}_t, t) \quad (24)$$

$$= \epsilon_\theta(\mathbf{x}_t, c, t) + w(\epsilon_\theta(\mathbf{x}_t, c, t) - \epsilon_\theta(\mathbf{x}_t, t)) \quad (25)$$

$$= \epsilon_\theta(\mathbf{x}_t, c, t) + wC \quad (26)$$

We can clearly see that  $C$  stands for classification information as mentioned in [15]. Replace the  $\tilde{\epsilon}$  to Eq.10, we have:

$$\mathbf{x}_{t-1} = \mathbf{x}_t - \underbrace{\left(\frac{\sqrt{\alpha_t} - 1}{\sqrt{\alpha_t}} \mathbf{x}_t + \frac{1 - \alpha_t}{\sqrt{1 - \alpha_t} \sqrt{\alpha_t}} \epsilon_\theta(\mathbf{x}_t, c, t) - \sigma_t \mathbf{z}\right)}_{\text{Original denoising framework}} - \underbrace{\frac{\alpha_t - 1}{\sqrt{1 - \alpha_t}} wC}_{\text{classification information}} \quad (27)$$

From this derivation, we can further apply the technique from CompG to the classification term in classifier-free guidance.

## G Related work

Diffusion Generative Models (DGMs) [6, 16–18] have recently become one of the most popular generative models in many tasks such as image editing[19, 20], text-to-image sampling [10] or image generation. Guidance is often utilized to improve the performance of DGMs [2, 1, 3–5]. Besides improving the performance, the guidance also offers a trade-off between image quality and diversity [], which helps users tune their sampling process up to their expectations. Although guidance is beneficial in many forms, it faces extremely serious drawbacks of running time. For classifier guidance, the running time is around 80% higher compared to the original diffusion model sampling time due to the evaluation of gradients at every sampling step. In contrast, classifier-free guidance requires the process to forward to the expensive diffusion model twice at every timestep.

Previous works on improving the running time of DGMs involve the reduction of sampling steps [21, 22] and latent-based diffusion models [10, 8]. Recently, the research community has focused on distilling from a large number of timesteps to a smaller number of timesteps [23–25] or reducing the architectures of diffusion models [25]. However, most of these works mainly solve the problem of the expensive sampling of diffusion models. As far as we notice, none of the works have dealt with the exorbitant cost resulting from guidance.

## H Additional qualitative results

Table 11: All hyper-parameters required for reproducing the results.

MODEL	DATASET	$k$	$s$	$ G $	TIME-STEPS
TABLE 2					
ADM	IMAGENET 64X64	1.0	0.0	0	250
ADM-G	IMAGENET 64X64	1.0	4.0	250	250
ADM-COMPG	IMAGENET 64X64	1.0	17.0	50	250
ADM	IMAGENET 256X256	1.0	0.0	0	250
ADM-G	IMAGENET 256X256	1.0	4.0	250	250
ADM-COMPG	IMAGENET 256X256	1.0	17.0	50	250
TABLE 3					
CADM	IMAGENET 64X64	1.0	0.0	0	250
CADM-G	IMAGENET 64X64	1.0	0.5	250	250
CADM-COMPG	IMAGENET 64X64	1.0	2.0	50	250
CADM-CFG	IMAGENET 64X64	1.0	0.1	250	250
CADM-COMPCFG	IMAGENET 64X64	1.0	10.0	25	250
CADM	IMAGENET 128X128	0.9	0.0	0	250
CADM-G	IMAGENET 128X128	1.0	0.5	250	250
CADM-CFG	IMAGENET 128X128	1.0	3.0	250	250
CADM	IMAGENET 256X256	1.0	0.0	0	250
CADM-G	IMAGENET 256X256	1.0	0.5	250	250
CADM-COMPG	IMAGENET 256X256	1.0	2.0	50	250
DiT-CFG	IMAGENET 256X256	1.0	1.5	250	250
DiT-COMPCFG	IMAGENET 256X256	1.0	6.0	22	250
TABLE 4					
GLIDE-G	MSCoco 64x64	1.0	0.0	250	250
GLIDE-COMPG	MSCoco 64x64	1.0	8.0	25	250
GLIDE-G	MSCoco 256x256	1.0	0.0	250	250
GLIDE-COMPG	MSCoco 256x256	1.0	5.5	35	250
TABLE 4					
SDIFF-CFG	MSCoco 64x64	1.0	2.0	250	250
SDIFF-COMPCFG	MSCoco 64x64	1.0	8.0	8	250

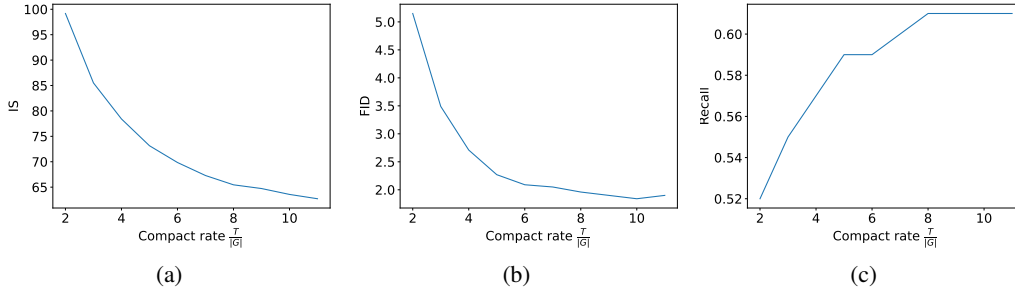
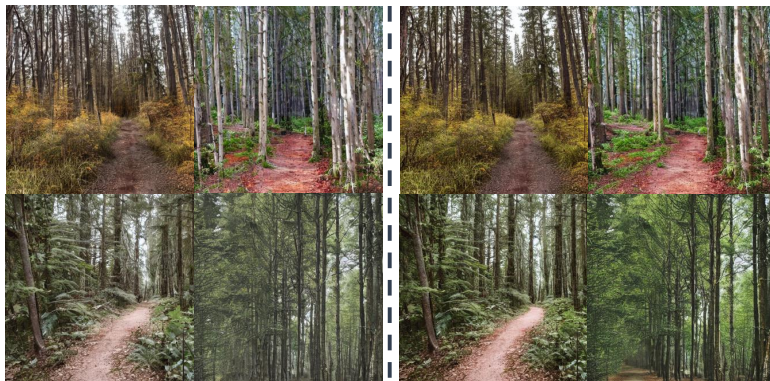
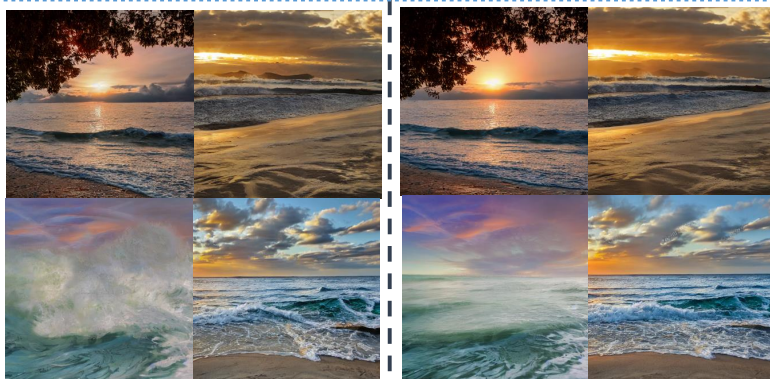


Figure 6: Trade-off: Running time versus performance. We measure the compact rate as  $\frac{T}{|G|}$ . In (a), IS decreases with increasing compact rate, while FID and Recall improve. However, when the rate exceeds 10, FID begins to rise. This suggests that increased diversity from more features initially enhances Recall and FID, but excessive diversity degrades image quality.

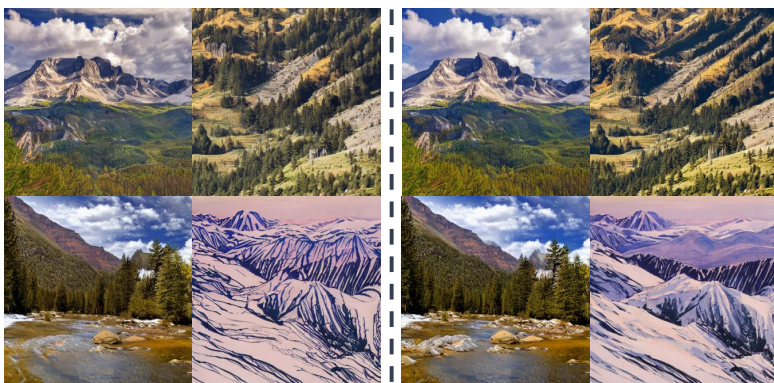
Quiet forest path surrounded by tall trees.



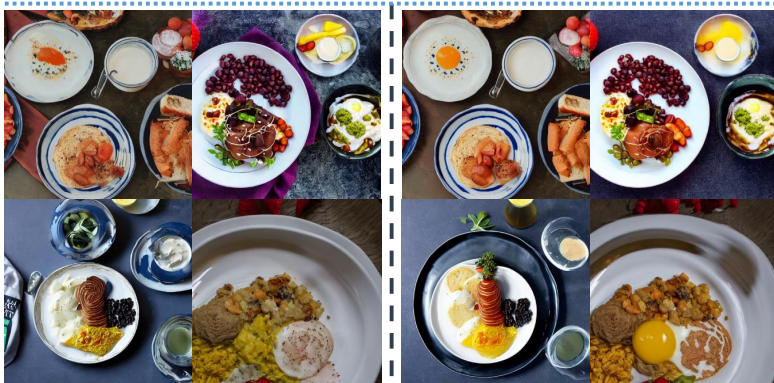
Beach at sunset with waves gently crashing.



Serene mountain landscape with a clear sky



A white plate with breakfast foods on it



StableDiffusion

(ours)

Figure 8: *Stable Diffusion with classifier-free guidance. The left figure is the vanilla classifier-free guidance with application on all 50 timesteps. Our proposed Compress Guidance method is the right figure, where we only apply guidance on 10 over 50 steps. The output shows our methods' superiority over classifier-free guidance regarding image quality, quantitative performance and efficiency.*



Flowers are arranged in a vase sitting on a table.



A plate with food on it, a fork and some kind of drink



StableDiffusion

(ours)

Figure 9: *Stable Diffusion with classifier-free guidance. The left figure is the vanilla classifier-free guidance with application on all 50 timesteps. Our proposed Compress Guidance method is the right figure, where we only apply guidance on 10 over 50 steps. The output shows our methods' superiority over classifier-free guidance regarding image quality, quantitative performance and efficiency.*

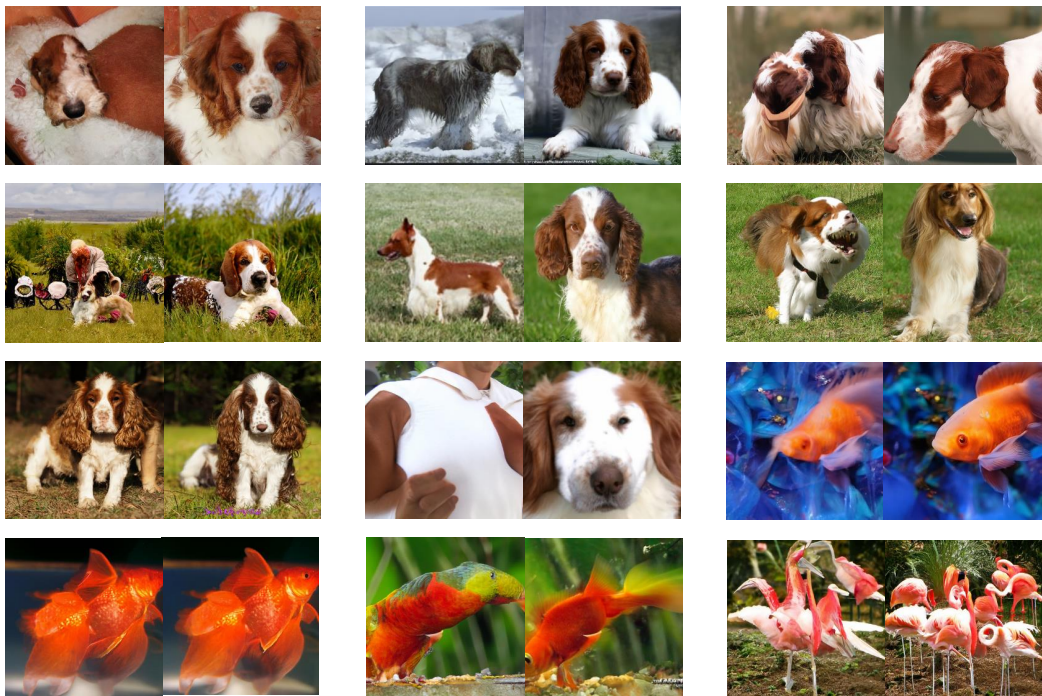


Figure 10: *Qualitative comparison between ADM-G and ADM-CompG. The image generated by ADM-G and ADM-CompG are put side by side. On the left side is ADM-G and on the right side is ADM-CompG.*



Figure 11: Images generated by DiT-CompCFG. From top to bottom classes goldfish, Welsh springer spaniel, Pembroke Welsh corgi, Cardigan Welsh corgi.



Figure 12: Images generated by DiT-CompCFG. From top to bottom classes redfox, kitfox, Arctic fox, tabby cat.